

¹ **Estimated likelihood of observing a large earthquake on a
2 continental low-angle normal fault, and implications for
3 low-angle normal fault activity**

Richard H. Styron¹ and Eric A. Hetland¹

Corresponding author: Richard H. Styron, Department of Earth and Environmental Sciences, University of Michigan, 2534 CC Little Bldg., 1100 N. University Ave., Ann Arbor, MI 48104, USA
(richard.h.styron@gmail.com)

¹Department of Earth and Environmental Sciences, University of Michigan, Ann Arbor, Michigan, USA.

4 The lack of observed continental earthquakes that clearly occurred on low-
5 angle normal faults (LANFs) may indicate that these structures are not seismi-
6 cally active, or that these earthquakes are simply rare events. To address this,
7 we compile all potentially active continental LANFs (twenty in total) and cal-
8 culate the likelihood of observing a significant earthquake on them over peri-
9 ods of 1-100 years. This probability depends on several factors including the
10 frequency-magnitude distribution. For either a characteristic or Gutenberg-Richter
11 distribution, we calculate a probability of about 0.5 that an earthquake greater
12 than $M6.5$ (large enough to avoid ambiguity in dip angle) will be observed on
13 any LANF in a period of 35 years, which is the current length of the Global CMT
14 catalog. We then use Bayes' Theorem to illustrate how the absence of observed
15 significant LANF seismicity over the catalog period moderately decreases the
16 likelihood that the structures generate large earthquakes.

1. Introduction

17 Low-angle normal faults (LANFs), with dips less than 30° , are well described in the geologic
18 record. They are thought to play an important role in accommodating large-magnitude conti-
19 nental extension [*Howard and John*, 1987] and crustal thinning [*Lister et al.*, 1986], and their
20 recognition has been a major development in continental tectonics [Wernicke, 2009]. However,
21 despite widespread field observations of inactive LANFs and their central role in extensional
22 tectonic theory, they remain enigmatic and contentious structures, and it is not clear if they are
23 seismically active at low dip angles in the upper crust. This is for two reasons: because brittle
24 faulting on LANFs is in apparent conflict with standard Andersonian rock mechanical theory as
25 typically applied to the upper crust [Axen, 2004], and because observations of active faulting on
26 LANFs are sparse and at times ambiguous [Wernicke, 1995]. A considerable amount of research
27 has been performed to address the former concern, reconciling LANF slip with rock mechanics
28 [e.g., Axen and Bartley, 1997; Collettini, 2011]. The latter issue is highlighted by studies that
29 have searched the focal mechanism catalogs and found no normal faulting earthquakes with
30 focal mechanisms and surface ruptures clearly indicating slip on planes $\leq 30^\circ$ [Jackson, 1987;
31 Collettini and Sibson, 2001], which is taken as conclusive evidence that LANFs are inactive
32 or aseismic. However, the lack of observed seismic slip on continental LANFs may be simply
33 because they are rare structures with long recurrence intervals, so earthquakes on them are very
34 infrequent. Without knowing the likelihood of observing an LANF rupture in a time window of
35 a few decades, it is not clear if an empty search result is strong evidence against LANF seismic-
36 ity. If this likelihood is known, though, Bayesian probability theory provides a framework for
37 quantifying how the negative search results impact the probability that LANFs are seismogenic.

38 In this work, we estimate the maximum likelihood of a significant LANF event occurring
39 in time windows from 1 to 100 years, and then we interpret the lack of observed LANF seis-
40 micity in a quantified, probabilistic context using Bayes' Theorem. We estimate the maximum
41 observation likelihood by treating all potentially active LANFs described in the literature as
42 seismically active at their surface dip angles throughout the upper crust. Under these assump-
43 tions, we create synthetic earthquake catalogs with both Gutenberg-Richter and 'characteristic'
44 frequency-magnitude distributions, using each fault's geometry and slip rate. We then calculate
45 the probability of observing earthquakes on at least one LANF over different observation peri-
46 ods. Finally, we use Bayes' Theorem to incorporate the negative catalog search results and the
47 observance likelihood to show how the negative results reduce the probability that LANFs are
48 seismically active, but do not bring the final probability to zero.

1.1. LANF Slip, Mohr-Coulomb Failure Theory, and Earthquakes

49 Areas of the crust undergoing active extension are generally assumed to have a subvertical
50 maximum compressive stress. Mohr-Coulomb theory, as applied to the crust, predicts that a
51 fault with a typical coefficient of friction for rocks (0.6–0.8) should lock up if it is oriented at
52 an angle greater than 60° to the maximum compressive stress (*i.e.*, fault dips less than 30°), and
53 new, optimally oriented faults should form [Sibson, 1985]. Therefore, for normal faults with
54 dips less than 30° , either much lower fault friction or elevated pore fluid pressure is required for
55 fault slip.

56 Evidence for seismic slip on LANFs is sparse. This is partly due to the ambiguity of the
57 rupture plane in earthquake focal mechanisms, as a focal mechanism with a low angle nodal
58 plane will also by definition have a high angle nodal plane. Without ancillary information

59 indicating which nodal plane corresponds to the slip surface, searches of earthquake catalogs
60 cannot yield unique results as to whether they contain LANF events. Several collections of
61 normal fault earthquakes with known surface breaks [Jackson, 1987; Collettini and Sibson,
62 2001], thereby resolving dip ambiguity, contain no low-angle events, although we note the total
63 number of events in these collections are small (\leq 25 events). Some candidate LANF events
64 exist, but they are undersea [e.g., Abers, 2001] or difficult to verify [e.g., Doser, 1987].

2. Potentially Active LANFs

65 Over the past decade or so, many field studies have found evidence for LANF activity in
66 orogens throughout the world. These studies typically find arrays of Quaternary normal fault
67 scarps on the fault traces and/or in the hanging walls of mapped or inferred low-angle detach-
68 ment faults [e.g., Axen *et al.*, 1999]. Some studies also have bedrock thermochronology data
69 from the exhumed detachment footwalls that are suggestive of ongoing rapid exhumation [e.g.,
70 Sundell *et al.*, 2013], although this data does not preclude a recent cessation of faulting. In
71 some cases, additional evidence for LANF activity comes from geophysical data such as GPS
72 geodesy [e.g., Hreinsdóttir and Bennett, 2009] and seismic waves [e.g., Doser, 1987].

73 We have compiled all potentially active LANFs with known subareal fault traces from a thor-
74ough review of the literature, finding twenty total (Figure 1). We have then mapped the ap-
75 proximate fault traces into a GIS file (available at https://github.com/cossatot/LANF_gis), with
76 metadata such as slip rate and source. Though the fault traces of many LANFs considered here
77 are obscured by vegetation, others display large fault scarps in Quaternary sediments, particu-
78 larly those in Tibet [e.g., Styron *et al.*, 2013; Kapp *et al.*, 2005] and the western US [e.g., Axen
79 *et al.*, 1999; Hayman *et al.*, 2003], which are commonly interpreted as evidence for past seismic

slip. About half are in Tibet, consistent with hypotheses that LANFs and metamorphic core complexes form in areas of hot, thick crust [e.g., *Buck*, 1991]. The rest are distributed through other areas of active continental extension: the North American Basin and Range, the Malay Archipelago, western Turkey, Italy, and Peru.

Several of the most-commonly cited candidates for seismically active LANFs were not included because they do not have a clearly-defined, mappable fault trace, which is necessary for our earthquake likelihood calculations. These include the 1995 Aigion, Greece earthquake fault [Bernard *et al.*, 1997] and other potential LANFs underneath the Gulf of Corinth, and the 1952 Ancash, Peru earthquake fault [Doser, 1987]. Though submarine core complexes with superficially low-angle detachments are well-described in the literature and some of these structures may have produced recent earthquakes [Abers, 2001], we do not include these in our calculations for several reasons: because mid-ocean ridges have not been structurally mapped with the completeness or resolution of subareal extensional provinces, it is not currently possible to come up with a reasonably complete inventory of ocean LANFs; without high-resolution structural mapping and geodesy of oceanic LANFs, it is not possible to determine which structures in a mid-ocean ridge segment are currently active (seismically or not), and it is difficult to confidently associate particular earthquakes with a specific fault, given the high spatial density of normal faults at mid-ocean ridges.

3. Likelihood of observing an LANF event

3.1. Earthquake Likelihood on Individual LANFs

To estimate the likelihood of observing a significant earthquake on an individual LANF over some contiguous time window of length t (in years), we perform a Monte Carlo simu-

100 lation in which we create 4000 synthetic time series of earthquakes, with unique values for
101 fault geometry and slip rate for each time series. Then, for each time series we calculate
102 the fraction of unique time windows of length t in which an earthquake as large or larger
103 than a given magnitude occurs. We take this value as the probability of observing an earth-
104 quake greater than or equal to moment magnitude M over time period t , which we will re-
105 fer to in general as $P(M,t)$. All calculations are performed with Python, using the Numpy
106 [Oliphant, 2007], IPython [Pérez and Granger, 2007], Pandas [McKinney, 2010], and Joblib
107 Parallel [Varoquaux and Grisel, 2009] packages. All code and data for this project is available
108 at https://github.com/cossatot/lanf_earthquake_likelihood/.

109 The geometry for each fault is estimated based on the length of the fault trace, the dip of the
110 fault, and the estimated fault locking depth in the area. The fault is treated as planar for simplic-
111 ity of calculations, even though the exposed footwalls of many detachment faults are nonplanar.
112 We determine the fault length by measuring the approximate length of the mapped fault trace
113 perpendicular to the assumed extension direction; for faults that change dip significantly along
114 strike, we only consider the low-angle segments of the fault. Values for the dip are taken from
115 the literature in most cases, and measurements of the dip of footwall triangular facets (inter-
116 preted as the exhumed fault plane) from SRTM data otherwise. In all cases, ranges of fault
117 geometries are considered, encompassing the degree to which the values are known. The fault
118 locking depth is assumed to be 10 km in the absence of other evidence (such as a geodetic study,
119 [e.g., Hreinsdóttir and Bennett, 2009]).

120 Slip rates of the 20 LANFs are gathered from the literature if possible, or given broad ranges
121 if not (e.g., 1–10 mm yr⁻¹). In the Monte Carlo simulation, samples for slip rate and dip are

¹²² drawn from uniform distributions defined by the maximum and minimum values. Based on
¹²³ field observations, some faults have dip ranges that go above 30°, although for these faults dip
¹²⁴ values are sampled from the minimum to 30°, as here we only consider slip on faults shallower
¹²⁵ than 30°. The resulting probabilities on these faults are then multiplied by the fraction of the
¹²⁶ dip range that is $\leq 30^\circ$.

¹²⁷ Each synthetic earthquake sequence is generated by randomly sampling either 50,000 events
¹²⁸ from a tapered Gutenberg-Richter (GR) distribution with corner magnitude $M_c = 7.64$ and
¹²⁹ $\beta = 0.65$ (from values estimated by *Bird and Kagan* [2004] for continental rifts), or a 25,000
¹³⁰ events from ‘characteristic’ distribution. It is not certain which distribution more appropri-
¹³¹ ately describes seismicity on a single LANF, though studies of many individual fault rup-
¹³² ture histories suggests that the characteristic distribution is more accurate [e.g., *Hecker et al.*,
¹³³ 2013]. The smaller number of samples drawn from the characteristic distribution is due to
¹³⁴ the increased computation time associated with a higher proportion of large events, leading to
¹³⁵ much longer time series for a given number of events. The samples are taken from an interval
¹³⁶ $M = [5.0, M_{max}]$, where M_{max} is the moment magnitude associated with 15 m of slip over the
¹³⁷ given fault plane. We use the standard relations between fault slip, D , and moment magnitude,
¹³⁸ M , given by

$$M_o = \mu L z D / \sin \delta \quad (1)$$

¹³⁹ and

$$M = 2/3 \log_{10}(M_o) - 6 \quad (2)$$

where L is the fault length, z is the seismogenic thickness, δ is the fault dip, $\mu = 30$ GPa is the shear modulus, and M_o is the seismic moment in N m [e.g., *Aki and Richards*, 2002; *Kagan*, 2003]. The characteristic distribution has a large-magnitude mode corresponding to $D = 1.5$ m on the fault, a typical slip distance for normal fault events [e.g. *Wesnousky*, 2008]. The distributions are shown in Figure 2.

These calculations rely on two important assumptions that warrant some discussion. The first is that each earthquake ruptures the entire fault patch uniformly. Though this is unlikely fault behavior, the long-term statistical distribution of earthquake recurrence is insensitive to assumptions about slip distribution in individual events as long as earthquakes are unclustered in time (the second assumption discussed below). Specifically, if n different, equal fault patches rupture independently, each requires n times the interseismic strain accumulation time to rupture with an earthquake of magnitude M compared to the accumulation time for a single fault rupturing uniformly with much lower coseismic slip in each earthquake. Thus, magnitude M events would happen with the same long-term frequency. The next assumption is that earthquakes are ordered randomly and separated by the time necessary for sufficient strain to accumulate for each earthquake to occur. This means that foreshock and aftershock sequences and other types of event clustering are not taken into account. However, the modal inter-event times for earthquakes $\geq M6$ or so are greater than a hundred years for most LANFs, so the ordering of events does not impact the results, as this is longer than our maximum observation window. Furthermore, any clustering resulting in event spacing less than the observation window would decrease $P(M, t)$, and here we choose to calculate the maximum $P(M, t)$ using the simplest as-

¹⁶¹ sumptions, rather than choose the model assumptions such that the calculated probabilities are
¹⁶² the minimum.

¹⁶³ The results for faults with a GR frequency-magnitude distribution indicate that it is unlikely
¹⁶⁴ that any individual fault would have an earthquake greater than $M 5$ in any observation time
¹⁶⁵ window up to 100 years. As an example, the results for the Panamint Valley fault are shown in
¹⁶⁶ Figure 3a; this fault has the highest $P(M, t)$ of any of the well-studied LANFs. The probability
¹⁶⁷ of observing a $\geq M 6.0$ event on the Panamint Valley fault is about 0.5 for $t = 100$ years, and
¹⁶⁸ about 0.15 for $t = 35$ years, which is the current length of the Global CMT catalog. As expected
¹⁶⁹ given the GR distribution, $P(M, t)$ is much higher for smaller, more frequent events than for
¹⁷⁰ larger events.

¹⁷¹ The results for faults with a characteristic frequency-magnitude distribution yield much lower
¹⁷² $P(M, t)$ for small to moderate events, but $P(M, t)$ is higher for large events(Figure 3b,d); this is
¹⁷³ because the earthquake sequences are dominated by large, infrequent events, so the inter-event
¹⁷⁴ times for moderate events are several times greater. For the Panamint Valley fault, $P(M \geq 5, t =$
¹⁷⁵ 35) is about 0.07 (versus 0.25 for the GR distribution), but $P(M \geq 7, t = 35)$ is around 0.025
¹⁷⁶ (versus essentially zero for the GR distribution). As the characteristic distribution likely better
¹⁷⁷ represents earthquakes on an individual large fault, these results suggest that is very unlikely
¹⁷⁸ that we would expect to capture any significant seismicity on an single LANF in the focal
¹⁷⁹ mechanism catalogs. A similar conclusion was found by *Wernicke* [1995] based on a simple
¹⁸⁰ calculation, assuming perfectly repeating large earthquakes on an idealized fault.

3.2. Earthquake Likelihood on All LANFs

To calculate the probability of observing at least one earthquake on *any* of these LANFs during a given time period, we first assume that seismicity on each fault is independent and uncorrelated with seismicity on all other faults. This assumption is likely true for most faults, but may not be true for the few proximal faults, though it is unclear how these faults may interact such that an appropriate joint probability may be calculated. We determine the probability for each time window and minimum magnitude with the equation

$$P_{AT \text{ or } LP \text{ or } \dots \text{ or } DV} = 1 - (Q_{AT} \cdot Q_{LP} \cdot \dots \cdot Q_{DV}) \quad (3)$$

₁₈₁ where P_{AT} is the probability of observing an earthquake on a single LANF (e.g., the Alto-
₁₈₂ Tiberina fault), and $Q_{AT} = 1 - P_{AT}$. Equation (3) is the union of probabilities for non-mutually
₁₈₃ exclusive random events.

₁₈₄ The results of this calculation are shown in Figure 4 a and b. For the Gutenberg-Richter
₁₈₅ distribution, the likelihood of observing an LANF earthquake on *any* fault over a given obser-
₁₈₆ vation period is quite high. For example, $P(M, t)$ for $M \geq 6$ and $t = 35$ years is about 0.85, and
₁₈₇ for the smaller events is quite close to 1. This high likelihood suggests that given the model
₁₈₈ assumptions, we should expect to find such an earthquake in the focal mechanism catalogs,
₁₈₉ though because many $M6$ events are not surface-breaking [Hecker *et al.*, 2013], it might be
₁₉₀ difficult to unambiguously determine whether the high- or low-angle nodal plane slipped. For
₁₉₁ $M \geq 6.5$, the probability of observing an LANF earthquake is about 0.5, and the nodal plane
₁₉₂ ambiguity should be much less (*e.g.*, due to surface scarps or directivity effects). The results
₁₉₃ for the characteristic distribution are lower than the results for the GR distribution for smaller

194 events and higher for larger events, similar to the patterns seen in results for individual faults.
195 $P(M \geq 5.5, t = 35)$ through $P(M \geq 6.5, t = 35)$ are all close, about 0.4–0.5.

3.3. Bayesian adjustments of LANF earthquake likelihood

196 Because the earthquake focal mechanism catalog is much shorter than the repeat time for
197 moderate to large earthquakes on typical normal faults with mm yr^{-1} slip rates, catalog searches
198 yielding no results for a particular class of events cannot be definitive evidence that they do not
199 occur. Nevertheless, the absence of observations does provide some evidence against their
200 existence. Through Bayes' Theorem, we can use the probability of observing an event (*i.e.*,
201 $P(M, t)$) to calculate the likelihood that LANFs are active given the negative outcome of catalog
202 searches. In this manner, Bayes' Theorem gives an adjusted, posterior likelihood for a given
203 prior likelihood that LANFs are capable of generating large earthquakes. Different priors may
204 result from different evidence or assumptions, and are not likely to be constant through time
205 or among all researchers. We do not choose a specific prior for LANF activity; rather, we
206 calculate the posteriors over the range of prior probabilities from 0 (meaning no probability that
207 LANFs are seismically active) to 1 (meaning LANFs are absolutely seismically active). Here
208 $P(A)$ represents the prior probability for LANF seismic activity, and $P(O)$ is the probability of
209 a positive test result (observation of an LANF earthquake in a catalog search). The symbol ‘~’
210 indicates *not*, so $P(\sim A)$ is the probability that LANFs are inactive; $P(\sim A) = 1 - P(A)$. The
211 results of this study give us the probability of observing or not observing an LANF event
212 given LANF seismic activity, $P(O|A)$ and $P(\sim O|A) = 1 - P(O|A)$, respectively. $P(O|\sim A)$ is
213 the probability of observing a ‘false positive’, the incorrect identification of an LANF event,
214 when in fact LANFs are not active. The posterior $P(A|\sim O)$ is the likelihood that LANFs

²¹⁵ can generate large earthquakes given that no LANF events have been observed, through Bayes'
²¹⁶ Theorem

$$P(A| \sim O) = \frac{P(\sim O|A)P(A)}{P(\sim O|A)P(A) + P(\sim O| \sim A)P(\sim A)}. \quad (4)$$

²¹⁷ Figure 5 shows $P(A| \sim O)$ for $P(A) \in [0, 1]$, using values for $P(O|A)$ of 0.1, 0.5, and 0.8, and
²¹⁸ a likelihood of false positives $P(O| \sim A) = 0.01$. The likelihood of LANF seismicity decreases
²¹⁹ appreciably given a moderate $P(O|A)$, but does not decrease to zero. Low values of $P(O|A)$
²²⁰ yield posteriors that are almost unchanged from the priors; in other words, the fact that no LANF
²²¹ events have occurred does not change the prior assumptions that LANF events are not expected
²²² to occur. Additionally, for strong priors with values very close to 0 or 1, the posteriors are much
²²³ closer to the priors, which is to say that it takes much more evidence to change strongly-held
²²⁴ positions. For less strongly-held prior assumptions, the posterior probability that the LANFs are
²²⁵ active is reduced compared to what the prior assumptions are. For example, in the case of a prior
²²⁶ of 0.5 (meaning that there is a 50% chance that LANFs can generate large earthquakes), then
²²⁷ if $P(O|A) = 0.1$, then the posterior likelihood for LANF seismicity drops to ≈ 0.48 (Figure 5).
²²⁸ In this case, the fact that a catalog search results in no identified LANF earthquake is non-
²²⁹ informative. If $P(O|A) = 0.5$, the posterior drops to ≈ 0.34 , a moderate reduction. On the other
²³⁰ hand, if $P(O|A) = 0.8$, the posterior is ≈ 0.17 .

4. Discussion and Conclusions

²³¹ Our compilation of all known potentially active LANFs shows that they are fairly uncommon
²³² structures, yet they still may be found in areas currently undergoing extension. Almost all major
²³³ continental extensional regions are represented; notably, narrow, linear continental rifts, such as

234 the East African and Rio Grande rifts, do not seem to contain active LANFs. This compilation
235 may serve as a point of comparison for different characteristics of active normal faults or LANF
236 geometry, or as a reference for any further study of these structures.

237 Any value for $P(M, t)$ we calculate here is a maximum estimate. As discussed above, part of
238 the reason that $P(M, t)$ is the maximum is due to the fact that we assume declustered earthquake
239 catalogs. Additionally, $P(M, t)$ is a maximum estimate as we assume that all LANFs in this
240 study are seismically active throughout the upper crust at surface dip angles. It is quite possible
241 that some of these faults are not tectonically active at all. It is also possible that some or all of
242 these detachments may be seismically active but at dip angles $\geq 30^\circ$. For example, the Cañada
243 David detachment in Mexico may dip very steeply at seismogenic depths [*Fletcher and Spelz*,
244 2009]. Some of these may also be aseismic; the Alto-Tiberina fault appears to be creeping for
245 much of its down-dip extent [*Hreinsdóttir and Bennett*, 2009], and the neighboring Zuccale
246 inactive LANF has fault gouge suggestive of creep [*Collettini and Holdsworth*, 2004]. If any
247 individual fault is not seismically active at low angles, this reduces the total $P(M, t)$ for all
248 events.

249 $P(M \geq 6.5, t = 35) \approx 0.5$ for either frequency-magnitude distribution, and is a good reference
250 value as events in this range are likely to be surface-breaking, and which would resolve the slip
251 plane ambiguity inherent in earthquake focal mechanisms [*Hecker et al.*, 2013]. Given the
252 fact that no significant LANF earthquakes have been definitively documented, this probability
253 of an LANF earthquake occurring during a 35 year time window results in a lowering of any
254 prior assumption that LANFs are active, as long as that prior assumption is not a strongly-held
255 position. The magnitude of the decrease depends on the prior likelihood, and the decrease is

256 at most $\sim 15\%$ (from 0.5 to 0.35). This means that the current catalog length is much too
257 short to be used as strong evidence against LANF seismicity. $P(M \geq 6.5, t = 100)$ is near 0.8
258 for both GR and characteristic distributions; this value more strongly reduces the likelihood of
259 LANF seismicity, yet still does not yield a definitive negative conclusion. Therefore, results
260 of studies analyzing the dip distribution of earthquakes on continental normal faults [Jackson,
261 1987; Collettini and Sibson, 2001] should be interpreted as informative but not conclusive.
262 Furthermore, alternative mechanisms for LANF occurrence or slip such as aseismic creep [e.g.,
263 Collettini, 2011; Hreinsdóttir and Bennett, 2009], isostatic flexure [e.g., Wernicke and Axen,
264 1988], or extremely long seismic recurrence intervals [Wernicke, 1995] need not be invoked to
265 explain the lack of observed seismicity, though these mechanisms may indeed be valid or well
266 supported by other observations.

267 **Acknowledgments.** We thank Jon Spencer for a stimulating discussion that became the im-
268 petus for this study. Mike Taylor and Kurt Sundell provided valuable comments on a draft of
269 the manuscript.

References

- 270 Abers, G. A. (2001), Evidence for seismogenic normal faults at shallow dips in continental rifts,
271 *Geological Society, London, Special Publications*, 187(1), 305–318.
- 272 Aki, K., and P. G. Richards (2002), *Quantitative seismology: Theory and methods*, University
273 Science Books.
- 274 Axen, G. J. (2004), Mechanics of low-angle normal faults, in *Rheology and Deformation of the*
275 *Lithosphere at Continental Margins*, edited by G. D. Karner et al., pp. 46–91, Columbia Univ.

- 276 Press, New York.
- 277 Axen, G. J., and J. M. Bartley (1997), Field tests of rolling hinges: Existence, mechanical
278 types, and implications for extensional tectonics, *Journal of Geophysical Research*, 102(B9),
279 20,515–20.
- 280 Axen, G. J., J. M. Fletcher, E. Cowgill, M. Murphy, P. Kapp, I. MacMillan, E. Ramos-
281 Velázquez, and J. Aranda-Gómez (1999), Range-front fault scarps of the Sierra El Mayor,
282 Baja California: Formed above an active low-angle normal fault?, *Geology*, 27(3), 247–250.
- 283 Bernard, P., P. Briole, B. Meyer, H. Lyon-Caen, J.-M. Gomez, C. Tiberi, C. Berge, R. Cattin,
284 D. Hatzfeld, C. Lachet, et al. (1997), The ms= 6.2, june 15, 1995 aigion earthquake (greece):
285 evidence for low angle normal faulting in the corinth rift, *Journal of Seismology*, 1(2), 131–
286 150.
- 287 Bird, P., and Y. Y. Kagan (2004), Plate-tectonic analysis of shallow seismicity: Apparent bound-
288 ary width, beta, corner magnitude, coupled lithosphere thickness, and coupling in seven tec-
289 tonic settings, *Bulletin of the Seismological Society of America*, 94(6), 2380–2399.
- 290 Buck, W. R. (1991), Modes of continental lithospheric extension, *Journal of Geophysical Re-*
291 *search: Solid Earth (1978–2012)*, 96(B12), 20,161–20,178.
- 292 Collettini, C. (2011), The mechanical paradox of low-angle normal faults: Current understand-
293 ing and open questions, *Tectonophysics*, 510(3), 253–268.
- 294 Collettini, C., and R. Holdsworth (2004), Fault zone weakening and character of slip along low-
295 angle normal faults: insights from the Zuccale fault, Elba, Italy, *Journal of the Geological*
296 *Society*, 161(6), 1039–1051.

- 297 Collettini, C., and R. H. Sibson (2001), Normal faults, normal friction?, *Geology*, 29(10), 927–
298 930.
- 299 Doser, D. I. (1987), The Ancash, Peru, earthquake of 1946 november 10: Evidence for low-
300 angle normal faulting in the high andes of northern peru, *Geophysical Journal of the Royal
301 Astronomical Society*, 91(1), 57–71.
- 302 Fletcher, J. M., and R. M. Spelz (2009), Patterns of Quaternary deformation and rupture prop-
303 agation associated with an active low-angle normal fault, Laguna Salada, Mexico: Evidence
304 of a rolling hinge?, *Geosphere*, 5(4), 385–407.
- 305 Hayman, N. W., J. R. Knott, D. S. Cowan, E. Nemser, and A. M. Sarna-Wojcicki (2003), Qua-
306 ternary low-angle slip on detachment faults in Death Valley, California, *Geology*, 31(4), 343–
307 346.
- 308 Hecker, S., N. Abrahamson, and K. Wooddell (2013), Variability of displacement at a point:
309 Implications for earthquake-size distribution and rupture hazard on faults, *Bulletin of the
310 Seismological Society of America*, 103(2A), 651–674.
- 311 Howard, K. A., and B. E. John (1987), Crustal extension along a rooted system of imbricate
312 low-angle faults: Colorado River extensional corridor, California and Arizona, *Geological
313 Society, London, Special Publications*, 28(1), 299–311.
- 314 Hreinsdóttir, S., and R. A. Bennett (2009), Active aseismic creep on the Alto Tiberina low-angle
315 normal fault, Italy, *Geology*, 37(8), 683–686.
- 316 Jackson, J. (1987), Active normal faulting and crustal extension, *Geological Society, London,
317 Special Publications*, 28(1), 3–17.

- 318 Kagan, Y. Y. (2003), Accuracy of modern global earthquake catalogs, *Physics of the Earth and*
319 *Planetary Interiors*, 135(2), 173–209.
- 320 Kapp, J. L., T. M. Harrison, P. Kapp, M. Grove, O. M. Lovera, and D. Lin (2005), Nyainqnen-
321 tanglha Shan: a window into the tectonic, thermal, and geochemical evolution of the Lhasa
322 block, southern Tibet, *Journal of Geophysical Research: Solid Earth (1978–2012)*, 110(B8).
- 323 Lister, G., M. Etheridge, and P. Symonds (1986), Detachment faulting and the evolution of
324 passive continental margins, *Geology*, 14(3), 246–250.
- 325 McKinney, W. (2010), Data structures for statistical computing in python, in *Proceedings of the*
326 *9th Python in Science Conference*, edited by S. van der Walt and J. Millman, pp. 51 – 56.
- 327 Oliphant, T. E. (2007), Python for scientific computing, *Computing in Science & Engineering*,
328 9(3), 10–20.
- 329 Pérez, F., and B. E. Granger (2007), IPython: a System for Interactive Scientific Computing,
330 *Comput. Sci. Eng.*, 9(3), 21–29.
- 331 Sibson, R. H. (1985), A note on fault reactivation, *Journal of Structural Geology*, 7(6), 751–754.
- 332 Styron, R. H., M. H. Taylor, K. E. Sundell, D. F. Stockli, J. A. Oalmann, A. Möller, A. T.
333 McCallister, D. Liu, and L. Ding (2013), Miocene initiation and acceleration of exten-
334 sion in the South Lunggar rift, western Tibet: Evolution of an active detachment system
335 from structural mapping and (U-Th)/He thermochronology, *Tectonics*, 32(4), 880–907, doi:
336 10.1002/tect.20053.
- 337 Sundell, K. E., M. H. Taylor, R. H. Styron, D. F. Stockli, P. Kapp, C. Hager, D. Liu, and
338 L. Ding (2013), Evidence for constriction and Pliocene acceleration of east-west extension
339 in the North Lunggar rift region of west central Tibet, *Tectonics*, 32(5), 1454–1479, doi:

340 10.1002/tect.20086.

341 Varoquaux, G., and O. Grisel (2009), Joblib: Running Python function as pipeline jobs.

342 Wernicke, B. (1995), Low-angle normal faults and seismicity: A review, *Journal of Geophysical*
343 *Research*, 100(B10), 20,159–20.

344 Wernicke, B. (2009), The detachment era (1977–1982) and its role in revolutionizing continental
345 tectonics, *Geological Society, London, Special Publications*, 321(1), 1–8.

346 Wernicke, B., and G. J. Axen (1988), On the role of isostasy in the evolution of normal fault
347 systems, *Geology*, 16(9), 848–851.

348 Wesnousky, S. G. (2008), Displacement and geometrical characteristics of earthquake sur-
349 face ruptures: Issues and implications for seismic-hazard analysis and the process of earth-
350 quake rupture, *Bulletin of the Seismological Society of America*, 98(4), 1609–1632, doi:
351 10.1785/0120070111.

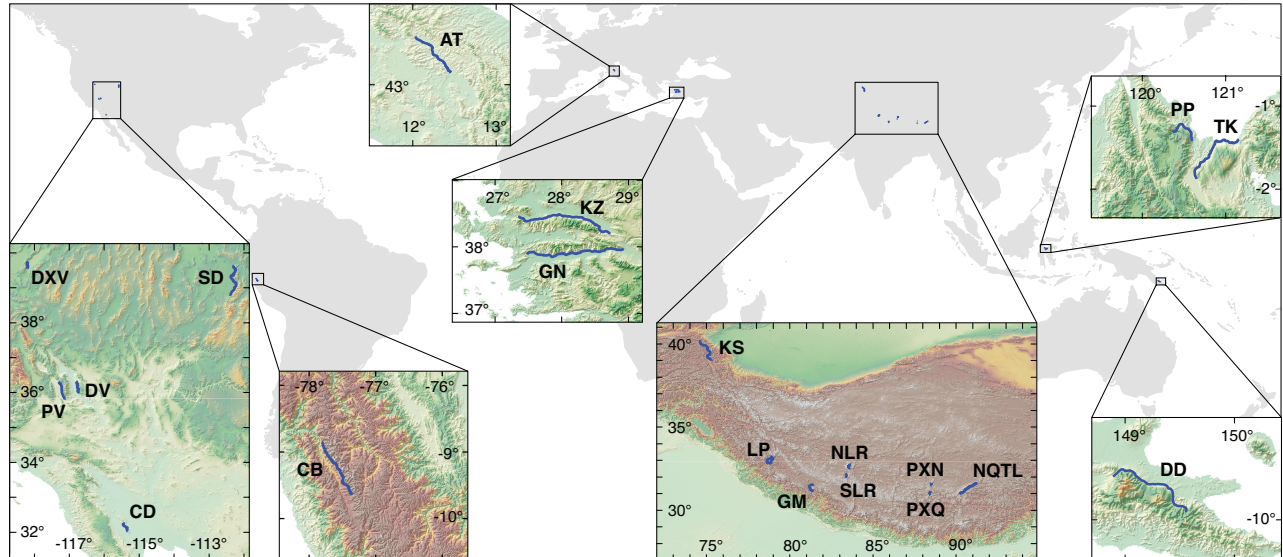


Figure 1. Map of known, potentially active continental LANFs (blue lines), with insets showing the physiographic context of the faults. DXV=Dixie Valley fault. PV=Panamint Valley fault. DV=Death Valley fault. CD=Cañada David detachment. SD=Sevier Desert detachment. CB=Cordillera Blanca detachment. AT=Alto-Tiberina fault. KZ=Kuzey detachment. GN=Guney detachment. KS=Kongur Shan fault. LP=Leo Pargil detachment. GM=Gurla Mandhata detachment. NLR=North Lunggar detachment. SLR=South Lunggar detachment. PXN=Pum Qu–Xainza north fault. PXQ=Pum Qu–Xainza Qingdu fault. NQTL=Nyainqentanglha detachment. PP=Pompangeo detachment. TK=Tokorondo detachment. DD=Dayman Dome.

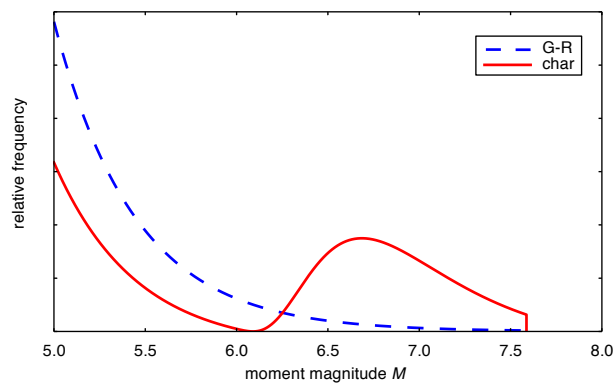


Figure 2. Gutenberg-Richter and characteristic frequency-magnitude distributions for the South Lunggar detachment

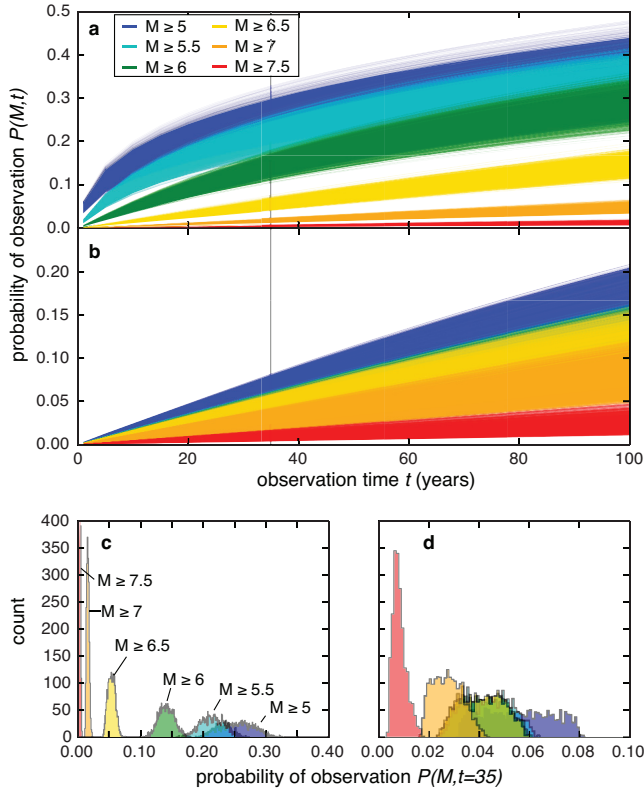


Figure 3. **a:** Probabilities of observing an earthquake greater than or equal to a given moment magnitude M over a given observation window on the Panamint Valley fault, for the Gutenberg-Richter distribution. **b:** Probabilities of observing an earthquake greater than or equal to a given moment magnitude M over a given observation window on the Panamint Valley fault, for the characteristic distribution. Note the change in the scale of the y axis. **c:** Cross-section through **a** at $t = 35$ years, showing the distributions of $P(M)$. **d:** Cross-section through **b** at $t = 35$ years, showing the distributions of $P(M)$.

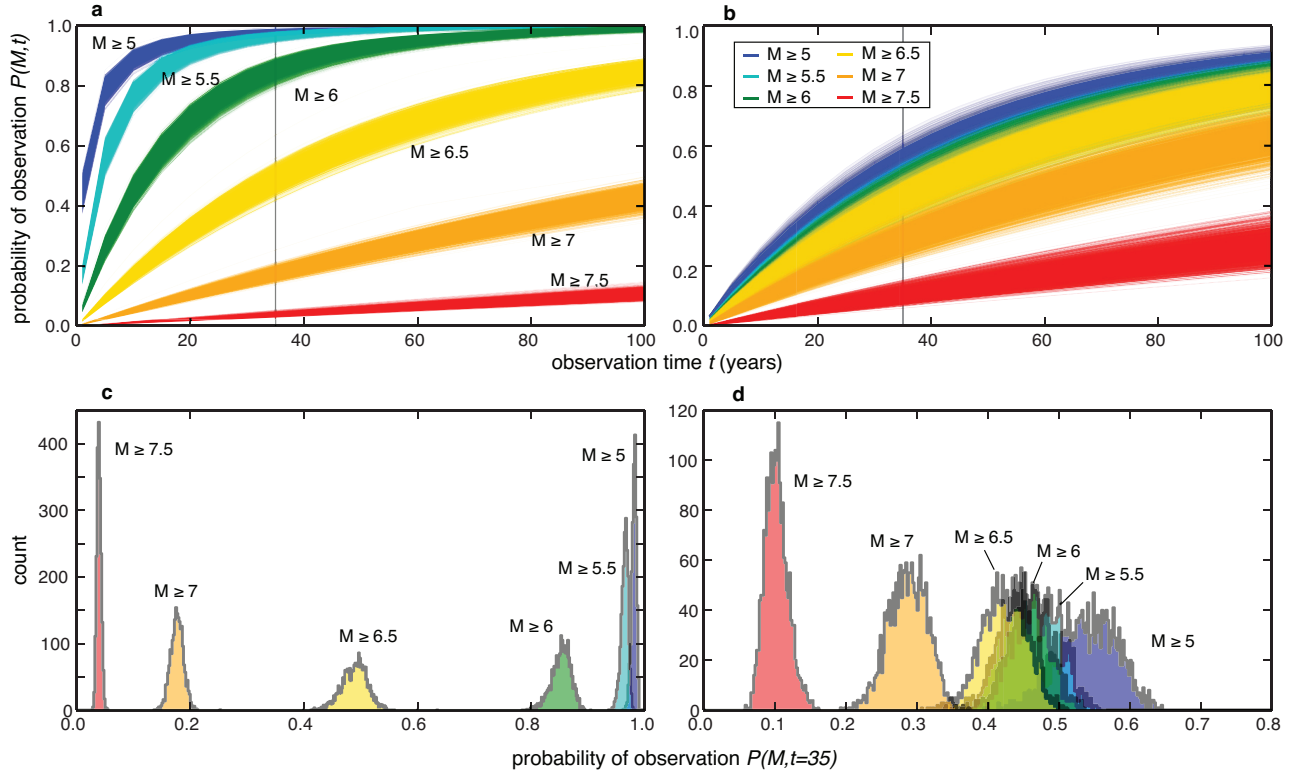


Figure 4. **a:** Probabilities of observing an earthquake greater than or equal to a given moment magnitude M over a given observation window on any LANF, given a Gutenberg-Richter distribution. **b:** Probabilities of observing an earthquake greater than or equal to a given moment magnitude M over a given observation window on any LANF, given a characteristic distribution. **c:** Cross-section through **a** at $t = 35$ years showing probability distributions. **d:** Cross-section through **b** at $t = 35$ years showing probability distributions.

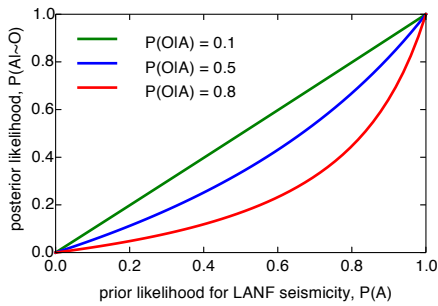


Figure 5. Prior likelihood for LANF seismicity $P(A)$ and posterior likelihood $P(A|O)$ given no observed earthquakes. $P(O|A)$ is the likelihood of observing an earthquake given activity on all LANFs.